RSC Advances

PAPER

View Article Online
View Journal | View Issue

Cite this: *RSC Adv.*, 2023, **13**, 30358

Development and characterization of novel emulsified nanocomposite coatings incorporating different loadings of nanoclay and beeswax for paper packaging

Hajer Aloui *[ab] and Khaoula Khwaldia [a]

Paper coated with poly (vinyl alcohol) (PVA)-based films incorporating varying amounts of halloysite nanotubes (HNTs) and/or beeswax (BW) were developed. The applied PVA/HNTs nanocomposite films, PVA/BW emulsified films, and PVA/HNTs/BW emulsified nanocomposite films were characterized in terms of FTIR, TGA, DSC, and XRD analyses. The effects of HNTs and/or BW at different loadings on the functional properties of coated paper were investigated. HNTs and BW co-incorporation significantly improved the water vapor permeability of the resulting PVA/HNTs/BW coated paper samples, and reduced their $Cobb_{60}$ values, respectively, by more than 50, 24, and 18% as compared to the uncoated paper, paper coated with pristine PVA and paper coated with PVA/HNTs nanocomposite-based coatings. While increasing their contact angle values in the range of 10–20%. Likewise, HNTs and BW co-incorporation increased the mechanical strength of PVA/HNTs/BW coated paper in the range of 20.54–29.80% as compared to the uncoated paper, while increasing their flexibility up to 32.50%. Such enhancement in the functional properties of PVA/HNTs/BW coated paper is most likely due to the establishment of interactions between PVA, BW, and HNTs. Our results demonstrate the ability of PVA/HNTs/BW emulsified nanocomposite coatings to improve paper barrier and mechanical properties owing to the prominent reinforcement effects of HNTs and the good moisture–barrier properties of BW.

Received 1st August 2023
Accepted 5th October 2023

DOI: 10.1039/d3ra05211g

rsc.li/rsc-advances

Introduction

Increasing public concerns over *environmental* damage caused by conventional plastic materials has drawn attention to the use of biodegradable materials to reduce waste disposal through biological recycling, with the aim of achieving a sustainable ecosystem.[1]

Paper is recognized as a safe and environmentally friendly material due to its biodegradability, renewability, and recyclability.[2] However, this cellulosic material exhibits a porous structure with high surface hydrophilicity,[1] which may affect its mechanical strength, especially in moist environments.[3] In this regard, the paper needs to be combined with other materials to improve its barrier properties and therefore overcome the limitation of its applicability as an efficient packaging material.

Coatings based on conventional polymers such as fluorocarbon, rubber latex, and polyethylene have shown great potential for improving the barrier properties of paper packaging material.[4] However, the *non-biodegradable* nature of *these synthetic layers* led to the loss of the inherent biodegradability and recyclability of the coated paper. In recent years, polyvinyl alcohol (PVA) has been gaining importance as a packaging material owing to its good film-forming ability, excellent gas barrier properties, chemical resistance, optical properties, and easy processability.[5] Moreover, PVA could be successfully used for paper coating applications due to its complete biodegradability.[6] However, PVA films have relatively high-water vapor permeability, low mechanical strength and thermal stability which may limit their application as coating materials. Recently, nanocomposite materials, created through dispersing nanoscale particles in polymer matrices, have attracted considerable research interest owing to the ability of the incorporated nanofillers to overcome some limitations mainly a poor water vapor barrier property, low mechanical resistance and thermal stability.[7–10] Among a large number of nanofillers, halloysite nanotubes (HNTs) have drawn particular attention as reinforcing nanomaterials owing to their high surface reactivity, large surface area, high mechanical strength, and relatively low cost.[11] Moreover, due to their unique nanotubular structure and relatively high hydrophilicity (Al–OH and Si–OH groups), HNTs have shown better dispersion in water-soluble polymeric matrices even at high loading contents without an exfoliation step, along with higher

[a]*Laboratoire des Substances Naturelles, Institut National de Recherche et d'Analyse Physico-chimique, Biotechpole Sidi Thabet 2020, Tunisia. E-mail: hajer.aloui@ymail.com; hajer.aloui@inrap.rnrt.tn*

[b]*Higher Institute of Biotechnology, Monastir (ISBM), Monastir, Tunisia*

cationic exchange capacity, which may promote hydrogen bond establishment between hydrogen atoms from PVA and oxygen atoms on HNTs.[12] Despite their ability, as reinforcing materials, to enhance the mechanical and thermal properties of different polymers,[12–15] the efficiency of HNTs in enhancing the barrier properties of the reinforced matrixes is still somehow limited due to their hydrophilic nature, which is mainly ascribed to the presence of permanent negative charges with attractive forces on water molecules.[15] Many researchers have attempted to improve the water barrier properties of bio-based films through hydrophobic compound addition, either in emulsion or in the form of a second layer applied over a previously formed film.[16–19] Among a variety of hydrophobic compounds, waxes have shown great potential in increasing the moisture resistance of bio-based films owing to their high hydrophobicity which is mainly associated with their high long-chain fatty alcohol and alkane content.[18] Beeswax (BW), mainly composed of wax esters, fatty acids, and hydrocarbons, has been successfully combined with biodegradable films to provide an efficient barrier to moisture. In this context, hydrophobic barrier coatings based on beeswax in combination with polysaccharides or proteins have shown great potential for improving the moisture resistance of coated paper. Previously, Sothornvit[20] reported a significant reduction in the water vapor permeability of hydroxypropyl methylcellulose-BW composite-coated paper. Likewise, Zhang *et al.*[21] underlined the efficiency of chitosan–BW-based coatings in improving the grease resistance and water vapor barrier of coated paper. Recently, Wang *et al.*[22] developed a waterproof coating based on beeswax-in-water Pickering emulsion using hemicellulose-grafted-lauric acid (H-LA) micelles as nano-stabilizers and reported the ability of this composite coating, when applied on the paper surface, to reduce water vapor permeability and increase contact angle values of coated paper. Despite their high moisture retention capacity as hydrophobic compounds, the incorporation of lipids and waxes into film-forming solutions may exert a weakening effect on the mechanical resistance of the polymeric matrix since interactions between polar polymers and waxes as nonpolar molecules are reported to be much lower than those between polar polymer molecules.[23] Recent studies have focused on the co-incorporation of nanofillers and hydrophobic compounds into film-forming solutions to fulfill requirements related to materials dedicated for food packaging applications through the combination of the prominent reinforcement effects of nanofillers and the good moisture–barrier properties of lipids. Although previous research has underlined the ability of nanofillers and hydrophobic compounds' co-incorporation to enhance the functionality of many hydrocolloid-based films,[24,25] until now, no study has focused on the effect of emulsified nanocomposite coatings' application on the functional properties of paper packaging materials. Thus, in this work, novel emulsified nanocomposite coatings based on PVA, HNTs and BW were applied to paper material, and the effect of HNTs and/or BW at different contents on the barrier and mechanical properties of coated paper was assessed.

Experimental

Materials

Paper packaging having the physical and mechanical properties detailed in Table 1 was kindly provided by SOTEFI (Soukra, Tunisia). PVA (99.2–99.7% hydrolyzed) with an average molecular weight of 89.000–98.000 Da was purchased from Sigma-Aldrich (Steinheim, Germany) to be used as a polymeric matrix for the incorporation of HNTs and BW. HNTs and BW, respectively, used as nanofillers and hydrophobic compounds, were obtained from Sigma Aldrich (Steinheim, Germany). The main physical properties of HNTs and BW are presented in Table 2.

Preparation of emulsified nanocomposite coating solutions

A pristine PVA coating solution (3% w/v) was prepared according to Aloui *et al.*[12] Briefly, 3 g of PVA powder was dispersed in

Table 1 Main physical and mechanical properties of paper-based material

Property	Unit	Mean value and standard deviation
Grammage	g m^{-2}	80.20 ± 0.12
Thickness	μm	99 ± 0.20
Mechanical properties		
Tensile strength	MPa	20.30 ± 1.48
Elongation at break	%	3.91 ± 0.29
Optical properties		
Opacity	%	93.24 ± 0.24
Whiteness	%	89.14 ± 0.20
$Gloss_{60}$	GU	3.63 ± 0.05
Barrier properties		
Water vapor permeability	g mm m^{-2} d^{-1} kPa^{-1}	38.25 ± 0.26
$Cobb_{60}$	g m^{-2}	42.63 ± 0.59
Contact angle	°	70.025 ± 0.88

100 mL of distilled water at 80 °C for 2 h under continuous stirring before being sonicated for 30 min to achieve complete polymer dispersion. Nanocomposite coating formulations were obtained by dispersing selected amounts of HNTs (6% and 12% w/w, based on PVA weight) in 100 mL of distilled water for 2 h. The resulting nanofillers dispersion was added to the PVA solution, and the mixture was continuously stirred for 1 h at room temperature before being sonicated for 2 h at 25 °C in an ultrasonic bath. Nanocomposite coating solutions were then sonicated at 3 pulse per s and an amplitude of 50% for 1 h using an ultrasonic probe (Sonics & Materials Inc., India) in the presence of an ice bath to control the temperature. BW was then added at 25 and 50 wt% (based on the total weight of the filmogenic solution). The resulting mixtures were sonicated for 30 min before being homogenized for 3 min at 21 500 rpm using an Ultra-Turrax T25 (IKA, Labortechnik GmbH, Munich, Germany) to obtain the emulsified nanocomposite coating solutions.

Coating procedure

A coating applicator (model KCC 101, RK Print-Coat Instruments, Hertz, UK) equipped with different standard wire-wound bars were used to provide a constant coating weight of 4 g m^{-2} on the paper surface through the application of nine different coating solutions. The composition of the different coating formulations is detailed in Table 3.

The coating process of the paper material was carried out at a speed of 4 m min^{-1}. After being dried and conditioned, coated paper sheets were characterized in terms of barrier and mechanical properties.

Table 2 Main physical properties of HNTs and BW. Source: data supplied by Sigma Aldrich

Compound	Property	Value
HNTS	Outer diameter	50 mm
	Inner diameter	15 nm
	Surface area	64 m^2 g^{-1}
	Pore volume	1.25 mL g^{-1}
	Refractive index	1.54
	Density	2.53 g cm^{-3}
BW	Melting point	62.0–65.0 °C
	Ester value	72–79
	Ratio ester/Acid	3.3–4.2

Characterization of emulsified, nanocomposite and emulsified-nanocomposite stand-alone coatings

Attenuated total reflectance Fourier-transform infrared (ATR-FTIR). Chemical interactions between PVA, BW, and HNTs were evaluated by ATR-FTIR spectroscopy. FTIR spectra were collected in a wave number range of 400 to 4000 cm^{-1}.

X-ray analysis. Wide-angle X-ray diffraction (WAXD) was carried out to assess the effect of different HNTs and BW loadings on the crystallinity of the PVA matrix using a Bruker D8-Advance (USA) diffractometer, as previously described by Aloui and Khwaldia.[26]

Thermogravimetric analysis. The effect of different HNTs and/or BW contents on the thermal stability of PVA matrix was assessed by thermogravimetric analysis (TGA) using a Discovery TGA (TGA 2950, TA Instruments). Experiments were performed at a temperature range of 25–1000 °C using a uniform heating rate of 10 °C min^{-1} under a helium atmosphere.

Differential scanning calorimetry (DSC) analysis. Differential Scanning Calorimetry (DSC) tests were performed using a TA DSC-Q1000 as previously described by Aloui and Khwaldia.[26]

The degree of crystallinity was calculated using the relationship:

$$X_c = \frac{1}{1 - m_f}\left[\frac{\Delta H}{\Delta H_0}\right] \times 100$$

where $(1 - m_f)$ is the weight fraction of PVA in the sample, ΔH, is the enthalpy for melting or crystallization, ΔH_0 is the enthalpy of melting for a 100% crystalline PVA sample, taken as 161.6 J g^{-1}.[26]

Characterization of coated paper

Water absorption assay ($Cobb_{60}$ method). Water absorption of paper samples was determined by the $Cobb_{60}$ method according to ISO 535.[27] Experiments were carried out using a Cobb tester (HK-213, Dongguan, China) allowing direct contact of a given amount of water with a test paper area for a specified time of 60 seconds. The amount of water absorbed by the cellulosic material was measured and expressed as g m^{-2}.

Table 3 Coating formulations' composition

Coating formulation	PVA concentration (% w/v)	HNTs content (% w/w, based on PVA weight)	BW content (% w/w, based on the total weight of the filmogenic solution)
Pristine PVA	3	0	0
PVA/6 HNTs	3	6	0
PVA/12 HNTs	3	12	0
PVA/25 BW	3	0	25
PVA/50 BW	3	0	50
PVA/6 HNTs/25 BW	3	6	25
PVA/6 HNTs/50 BW	3	6	50
PVA/12 HNTs/25 BW	3	12	25
PVA/12 HNTs/50 BW	3	12	50

Contact angle measurement. The wettability of the different coated paper samples was evaluated through contact angle measurement using a goniometer (Pocket goniometer PGX, Sweden) with distilled water droplet (5 μL) according to the sessile drop method as previously described by Aloui *et al.*[28]

Water vapor permeability (WVP). The WVP of the different coated paper samples was determined gravimetrically according to the ISO 2528 method.[29]

Tensile properties. A material testing machine (Lloyd LRX, Lloyd Instruments, Royston, UK) using a 0.5 kN static load cell was used to determine the tensile strength (TS) and elongation at break (% *E*) of the different coated paper samples according to ISO 1924-2-1994, as previously described by Khwaldia *et al.*[30]

Statistical analysis

Data were subjected to analysis of variance using Statgraphics® Plus 5.1 (Manugistics Inc., Rockville, MD, USA). Fisher's least significant difference (LSD) was used to compare samples, at the 95% confidence level. Differences between means were considered significant when the confidence interval is smaller than 5% ($p < 0.05$).

Results and discussion

ATR-FTIR analysis

To study the potential interactions between coating constituents, ATR-FTIR spectra of HNTs, pristine PVA film, PVA/6 HNTs nanocomposite film, PVA/25 BW emulsified film, and PVA/6 HNTs/25 BW emulsified nanocomposite film were recorded (Fig. 1).

As shown in Fig. 1, the HNTs spectrum displayed two absorbance bands at 3683 and 3612 cm^{-1}, respectively, assigned to the stretching vibration of the inner surface O–H groups that are connected to the aluminum-centered sheet, and to the stretching band of the inner groups.[31]

In addition to the bands explained above, the ATR-FTIR spectrum of the HNTs powder revealed the presence of two relevant peaks at 1004 and 907 cm^{-1} respectively, assigned to the stretching of Si–O network and Al–OH groups.[32] As can be inferred from the ATR spectrum of PVA/6 HNTs nanocomposite film, appreciable changes were observed upon the incorporation of HNTs. Overall, bands observed at 1004 and 907 cm^{-1} shifted toward higher wavelengths (respectively to 1027 and 920 cm^{-1}), which may suggest the establishment of hydrogen interactions between the OH groups of PVA and the oxygen atoms of Si–O bonds or the hydroxyl groups present on the surfaces of HNTs. Moreover, in the pristine PVA film spectrum, the FTIR peak at 3279 cm^{-1} assigned to O–H stretching shifted to 3290 cm^{-1} upon HNTs inclusion, which is mainly attributed to the establishment of strong interfacial interactions between the –OH groups located on HNTs surfaces such as silanol groups (–SiOH) and those from PVA molecules.[33–35] Additionally, the bands at 3683 and 3612 cm^{-1} related to Al_2OH of HNTs appeared in PVA/6HNTs nanocomposite films and shifted to higher frequencies (respectively to 3696 and 3624 cm^{-1}) denoting the presence of HNTs in the resulting nanocomposite film and their interaction with the PVA matrix. Likewise, a slight shift to higher frequencies (540 and 455 cm^{-1} respectively) was noticed for peaks located at 528 and 449 cm^{-1} and respectively assigned to the deformation of Al–O–Si and Si–O–Si groups of HNTs, confirming the formation of hydrogen-bonding interactions between PVA and HNTs. On the other hand, as compared to the pristine PVA film, the FTIR spectrum of PVA/25 BW emulsified film displayed two absorption bands specific to BW at 2850 and 1730 cm^{-1}, respectively, associated with the stretching vibration of C–H groups and the stretching vibration of saturated fatty ester bonds[36] indicating the successful incorporation of beeswax into the PVA matrix. As compared to the PVA/25 BW emulsified film, these two peaks slightly shifted toward lower frequencies in the FTIR spectrum of PVA/6HNTs/25BW emulsified nanocomposite film (respectively to 1721 and 2837 cm^{-1}), indicating the good miscibility between the PVA matrix and the incorporated HNTs and BW, mainly due to the formation of hydrogen bonds.

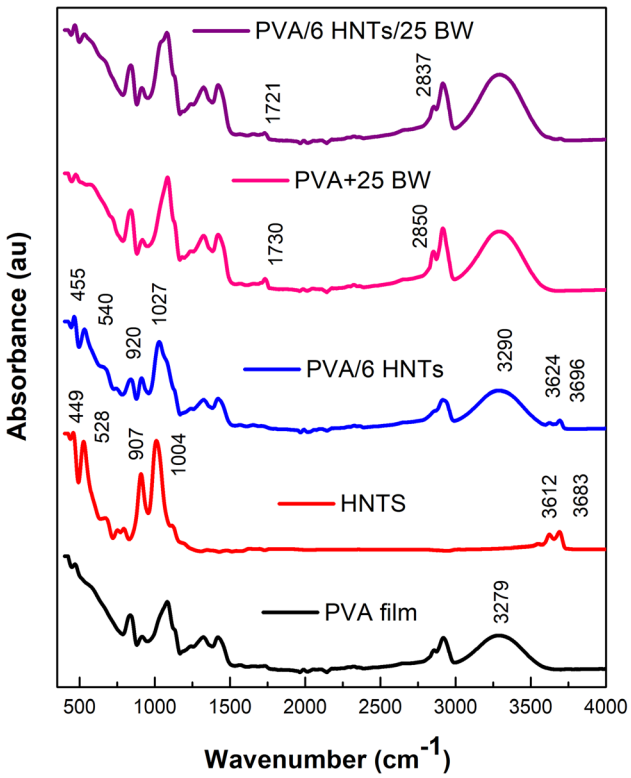

Fig. 1 FTIR spectra of HNTs, neat PVA film, PVA/6HNTs nanocomposite film, PVA/25BW emulsified film, and PVA/6HNTs/25BW emulsified nanocomposite film.

TGA analysis

TGA and derivative thermogravimetric (DTG) thermograms of the pristine PVA film, PVA/6 HNTs nanocomposite film, PVA/25 BW emulsified film and PVA/6 HNTs/25 BW emulsified nanocomposite film are presented in Fig. 2.

Overall, the pristine PVA film showed a multi-step thermal decomposition process. The first thermal degradation related to water evaporation was observed between 90 and 150 °C and

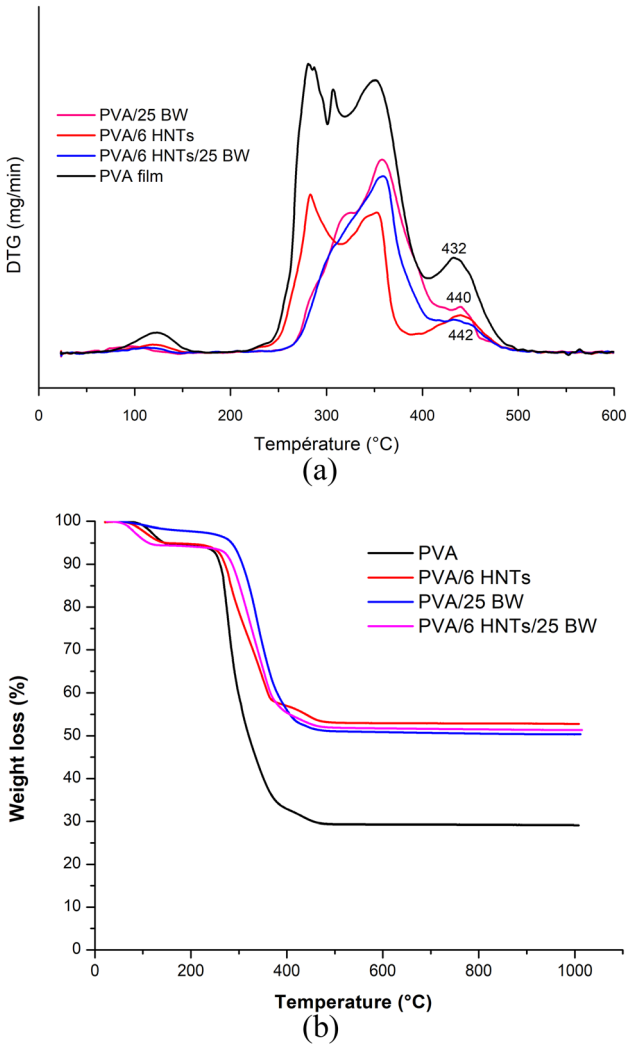

Fig. 2 (a) TG and (b) DTG curves of neat PVA film, PVA/6HNTs nanocomposite film, PVA/25BW emulsified film, and PVA/6HNTs/25BW emulsified nanocomposite film.

resulted in a weight loss of 0.5–5.15%. This first decomposition step was not detected for the PVA/25 BW emulsified film and the PVA/6 HNTs/25 BW emulsified nanocomposite film, probably due to their low moisture content arising from the hydrophobic nature of the incorporated beeswax. Similar behavior was noticed by Zhang *et al.*[37] for gelatin film incorporating either beeswax or carnauba wax. The second weight loss (5.81–67.13%) occurring at around 225–400 °C, was associated with the decomposition of the side chain of PVA. The third degradation step, occurring at around 436 °C with a weight loss of 70%, was attributed to cleavage of C–C backbone in the PVA main chain.[38] As can be inferred from Fig. 2, the peak associated with the C–C backbone cleavage in PVA shifted to a higher temperature at around 442 °C with a weight loss of 45.60% upon HNTs incorporation, suggesting an enhancement in the thermal stability of the resulting nanocomposite film. Likewise, Aloui *et al.*[12] and Abdullah *et al.*[33] have noticed the same tendency when HNTs were used as reinforcing materials for the PVA matrix. Such improvement in the thermal stability of the developed nanocomposite film can be explained by the homogeneous dispersion of HNTs in the polymeric matrix along with their efficiency as barriers against heat transfer inside the film.[12] Moreover, the hollow tubular structures of HNTs may delay mass transfer during the polymer degradation process owing to their ability to act as taps for volatile molecules, thus enhancing the thermal stability of the reinforced material traps for volatile particles.[39] On the other hand, as shown in Fig. 2, the thermal degradation of PVA/25% BW emulsified film and PVA/6HNTs/25% BW began above 250 °C, with an onset temperature of 275 °C indicating their higher thermal stability compared to the pristine PVA for which a lower onset temperature of 230 °C was recorded. Moreover, the DTG curve of the PVA/25 BW emulsified film showed an additional peak at around 325 °C, which is related to the degradation of beeswax.[37]

This result confirms the ability of beeswax to enhance the thermal stability of the PVA film. Previously, an increase in the thermal stability of gelatin films was noticed by Zhang *et al.*[37] when incorporating either BW or carnauba wax most likely due to the establishment of interactions between the wax fraction and the polar side groups in gelatin (such as amino, carbonyl and hydroxyl groups).

On the other hand, the peak at 432 °C associated with the C–C backbone cleavage in PVA shifted to higher temperatures at around 440 and 443 °C, respectively, for the PVA/25 BW emulsified film and the PVA/6 HNTs/25 BW nanocomposite film, with a weight loss of 47.73% and 47%, underlining the ability of BW either alone or in combination with HNTs to increase PVA thermal stability. This fact indicates the high level of compatibility between the different components of the polymeric blend that is believed to establish interactions (as confirmed by FTIR analysis), giving rise to more compact materials with enhanced thermal stability.

DSC analysis

Calorimetric curves related to the first heating scan of the pristine PVA film, PVA/6HNTs nanocomposite film, PVA/50 BW emulsified film, and PVA/6 HNTs/50 BW emulsified nanocomposite film are shown in Fig. 3, while the corresponding thermal data are presented in Table 4. As it can be inferred from Table 4, a decrease in the T_g of the PVA/HNTs nanocomposite film was observed as compared with the pristine PVA film, which is in agreement with Aloui *et al.*[12] findings. As previously emphasized by Liu *et al.*[40] the nanofiller geometry may play a critical role in the T_g of the resulting nanocomposite films. In fact, despite their nanometric diameter scale, HNTs length, which is between 1 and 15 μm is reported to be considerably higher than the typical gyration radii of polymer chains. Consequently, the polymer chains will be unable to completely wrap the nanotubes in three dimensions, leading to the appearance of many nanometric scale voids around the nanotubes that may create free volume between the chain segments, leading to a decrease in the T_g of the resulting nanocomposite material. Likewise, the incorporation of beeswax, either alone or in combination with HNTs, led to a decrease in the T_g of the PVA/50 BW emulsified film and the PVA/6 HNTs/50 BW

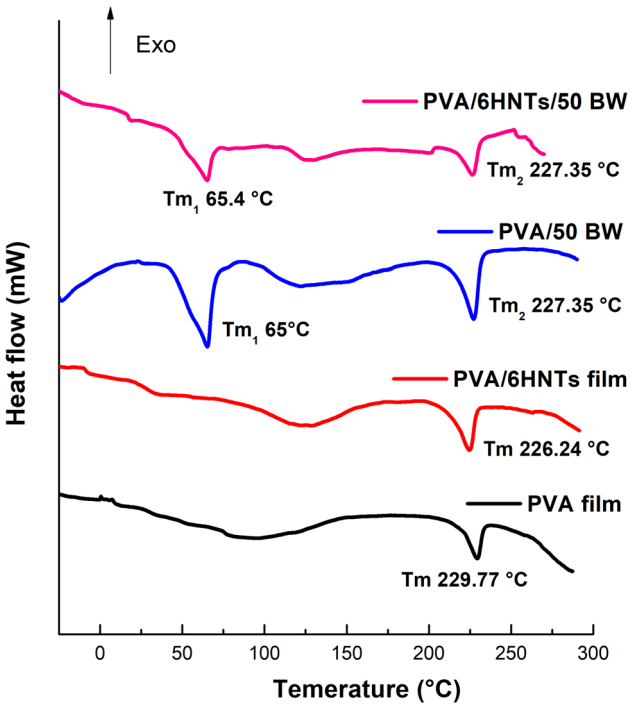

Fig. 3 DSC thermograms of neat PVA film, PVA/6HNTs nanocomposite film, PVA/50BW emulsified film, and PVA/6HNTs/50BW emulsified nanocomposite film.

emulsified nanocomposite film. Likewise, Abdul Haq *et al.*[41] noticed a decrease in the T_g of gum cordia film upon the incorporation of beeswax. According to these authors, such behavior is most likely attributed to the increase in polymer chain mobility upon beeswax incorporation. In fact, due to its plasticization effect, beeswax may impede interactions between polymer chains leading to an increase in the film matrix's mobility. As shown in Fig. 3, pure PVA film exhibited one endothermic peak corresponding to a melting temperature (T_m) of 229.77 °C. Overall, no significant change was noticed in the melting temperature of PVA/6 HNTs nanocomposite film as a result of HNTs incorporation, which corroborates with the previous findings of Aloui *et al.*[12] Concerning PVA/50 BW emulsified film and PVA/6 HNTs/50 BW emulsified nanocomposite film, a new endothermic peak associated with the solid–liquid transition of BW in the PVA matrix appeared in the vicinity of 65 °C which is in agreement with the melting point of BW usually occurring between 52 and 66 °C.[42] On the other hand, an increase of about 6% in the crystallization rate of PVA/6 HNTs nanocomposite film was noticed upon HNTs incorporation with respect to the pristine PVA film, which is in agreement with previous results of Aloui *et al.*[12] According to these authors, HNTs have the potential to increase the crystallization rate of polymeric matrices owing to their ability to act as effective nucleating seeds. As it can be inferred from Table 4, BW incorporation increased the crystallinity of both PVA/50 BW emulsified film and PVA/6 HNTs/50 BW emulsified nanocomposite film compared to the pristine PVA film. Previously, Kim *et al.*[43] noticed an increment in the crystallization rate of low-density polyethylene film upon paraffin wax incorporation.

X-ray diffraction analysis

The diffraction patterns of the pristine PVA film, PVA/6 HNTs nanocomposite film, PVA/50 BW emulsified film and PVA/6 HNTs/50 BW emulsified nanocomposite film are presented in Fig. 4. The pristine PVA film displayed a distinctive peak at $2\theta = 19.33°$, resulting from the strong hydrogen interactions between PVA chains.[12] As shown in Fig. 4, the diffraction pattern of PVA/6 HNTs film displayed an additional peak characteristic of the crystalline structure of HNTs at around $2\theta = 12°$, suggesting an increase in the crystallinity of the reinforced PVA film, which corroborates with DSC data that revealed a slight increase (6%) in the crystallization rate of PVA/6 HNTs nanocomposite film, with respect to the pristine PVA film.

The diffractogram of beeswax showed two intense peaks $2\theta = 21.51°$ (d-spacing 4.1232 nm) and 23.75° (d-spacing 3.7199 nm) characteristic of the orthorhombic crystal structure in BW.[44] The presence of these two peaks was noticed in the diffractograms of both PVA/50 BW emulsified film and PVA/6 HNTs/50 BW nanocomposite emulsified film, indicating an increase in their crystallinity. These findings are in agreement with DSC analysis, which revealed an increment of 5% and 35%, respectively, for PVA/50 BW emulsified film and PVA/6 HNTs/50 BW nanocomposite emulsified film compared to the pristine PVA film.

Characterization of coated paper

Water absorption assay (Cobb$_{60}$ method). The water absorption of the uncoated and coated paper samples was evaluated by the Cobb$_{60}$ method (Table 5).

As shown in Table 5, the uncoated paper sample showed the highest water absorbency (Cobb value of 42.63 ± 0.59 g m^{-2}), in relation to the hydrophilic character of cellulosic fibers (abundance of –OH groups) and the porous interfibrillar network that

Table 4 DSC data related to the first heating scan

Films	T_g (°C)	T_m (°C)		ΔH_m (J g^{-1})		X_m (%)
		1st peak	2nd peak	1st peak	2nd peak	
PVA	59.37	—	229.77	—	68.53	42.41
PVA/6 HNTs	52.17	—	226.24	—	58.80	49.24
PVA/50 BW	51.62	65	227.35	28.99	51.97	48.03
PVA/6 HNTs/50 BW	51.31	65.40	227.35	44.24	80.62	77.95

may allow higher water molecules to penetrate through the cellulosic material.[45] Regardless of HNTs and BW contents, the application of the different coatings on the paper surface significantly reduced the Cobb values of coated paper sheets as compared to the uncoated cellulosic material ($p < 0.05$) most likely due to the ability of the applied biopolymer coating formulations to impregnate the fibrous structure of the cellulosic material and fill the interfibrillar cellulose spaces, thus imparting a hindrance to water molecules absorption.[46] This fact was confirmed by SEM images (Fig. 5), where the interfibrillar spaces and porous structure of the uncoated cellulosic material (Fig. 5a) were found to be filled by the coating materials (Fig. 5b–f) which may explain in part the observed reduction in terms of water absorption of the different coated paper samples. Likewise, previous studies have attributed the decrease in water absorption of coated paper samples to the application of coating substances on the surface of the fiber cellulosic matrix and their ability to penetrate the cellulosic material and fill its porous structure.

On the other hand, ANOVA analysis revealed that the incorporation of HNTs at different loadings did not significantly improve the water performance of PVA/HNTs nanocomposite-coated paper samples with respect to paper coated with pristine PVA ($p > 0.05$) because of the hydrophilic nature of the incorporated nanofillers.[47]

Previously, Türe *et al.*,[48] noticed an increase in the $Cobb_{60}$ values of paperboards coated with wheat gluten (WG)/montmorillonite (MMT) multilayered films as compared to uncoated and WG-coated paperboards. This result was ascribed to the hydrophilic character of the clay layer along with the increase in thickness of the applied nanocomposite coating. Conversely, a significant decrease in the range of 50.24–55.57% was observed in $Cobb_{60}$ values of PVA/BW emulsified coated paper samples when BW content was increased from 25 to 50 wt% ($p < 0.05$) demonstrating the ability of BW as a hydrophobic compound to reduce the hydrophilicity of the PVA-based coatings. Previously, Bhardwaj *et al.*[45] underlined the efficiency of chitosan–BW coatings, when applied on the surface of different paper samples, in reducing their water absorption. Likewise, Liu *et al.*[49] noticed a significant improvement in the water resistance of paper coated with microcrystalline wax emulsion, for which a reduction of 54.3% in $Cobb_{60}$ value was recorded upon the application of 10 g m^{-2} coating load on the paper surface. Such an improvement in the water resistance of coated sheets was most likely ascribed to the strong hydrophobicity of the branched saturated hydrocarbons of C31-70 composing the microcrystalline wax. Regardless of their contents, the co-incorporation of HNTs and BW significantly reduced the water absorption of the emulsified nanocomposite-coated sheets as compared to the uncoated paper, paper coated with pristine PVA and paper coated with PVA/HNTs nanocomposite-based coatings ($p < 0.05$) most likely due to

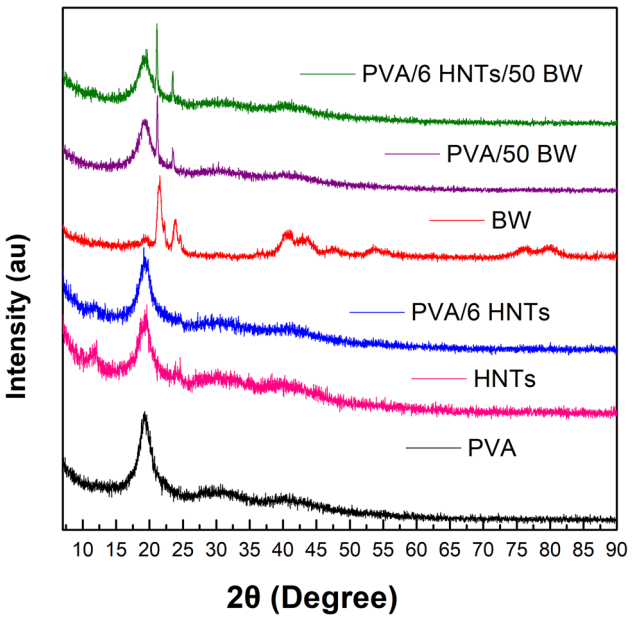

Fig. 4 XRD profile of neat PVA film, PVA/HNTs nanocomposite film, PVA/BW emulsified film, and PVA/HNTs/BW emulsified nanocomposite film.

Table 5 Thickness, barrier and mechanical properties of uncoated and coated papers[a]

Sample	Thickness (μm)	Water vapor permeability (g mm m^{-2} d^{-1} kPa^{-1})	Cobb (g m^{-2})	Contact angle (°)	Tensile strength (TS) (MPa)	Elongation at break (% *E*)
Uncoated paper	99 ± 0.20^{a}	38.25 ± 0.26^{a}	42.63 ± 0.59^{a}	70.025 ± 0.88^{a}	20.30 ± 1.48^{a}	3.91 ± 0.29^{a}
Paper coated with:						
PVA	102.50 ± 0.71^{b}	35.86 ± 0.25^{b}	28.05 ± 0.96^{b}	70.49 ± 0.96^{a}	23.11 ± 0.88^{b}	5.53 ± 0.11^{d}
PVA/6 HNTs	103.50 ± 0.71^{b}	36.12 ± 0.00^{b}	25.89 ± 0.74^{c}	71.17 ± 0.45^{a}	25.89 ± 1.15^{de}	5.33 ± 0.19^{cd}
PVA/12 HNTs	102.50 ± 0.30^{b}	36.61 ± 0.32^{ab}	27.21 ± 0.82^{bc}	71.26 ± 1.86^{a}	28.61 ± 1.16^{f}	5.26 ± 0.20^{bcd}
PVA/25 BW	102.50 ± 0.71^{b}	35.41 ± 1.38^{b}	21.21 ± 0.82^{d}	79.57 ± 1.28^{c}	23.77 ± 0.43^{bc}	5.46 ± 0.39^{d}
PVA/50 BW	103.50 ± 0.71^{b}	30.58 ± 0.21^{d}	18.94 ± 1.19^{e}	85.54 ± 2.17^{e}	23.97 ± 0.93^{bc}	5.26 ± 0.20^{bcd}
PVA/6 HNTs/25 BW	103.00 ± 1.41^{b}	33.31 ± 1.12^{c}	20.89 ± 0.96^{d}	77.10 ± 2.89^{b}	24.89 ± 1.29^{cd}	5.16 ± 0.24^{bc}
PVA/6 HNTs/50 BW	103.00 ± 1.00^{b}	32.18 ± 0.92^{cd}	18.91 ± 0.63^{e}	82.60 ± 2.62^{d}	24.47 ± 0.99^{c}	5.18 ± 0.31^{bc}
PVA/12 HNTs/25 BW	102.50 ± 1.29^{b}	35.24 ± 1.13^{b}	21.22 ± 0.42^{d}	82.34 ± 2.13^{d}	26.35 ± 0.68^{e}	5.08 ± 0.25^{bc}
PVA/12 HNTs/50 BW	102.25 ± 0.96^{b}	35.23 ± 1.13^{b}	20.89 ± 0.22^{d}	84.35 ± 2.73^{de}	25.78 ± 0.92^{de}	4.98 ± 0.27^{b}

[a] Different superscript letters (a–f) indicate significant differences among coating formulations ($p < 0.05$).

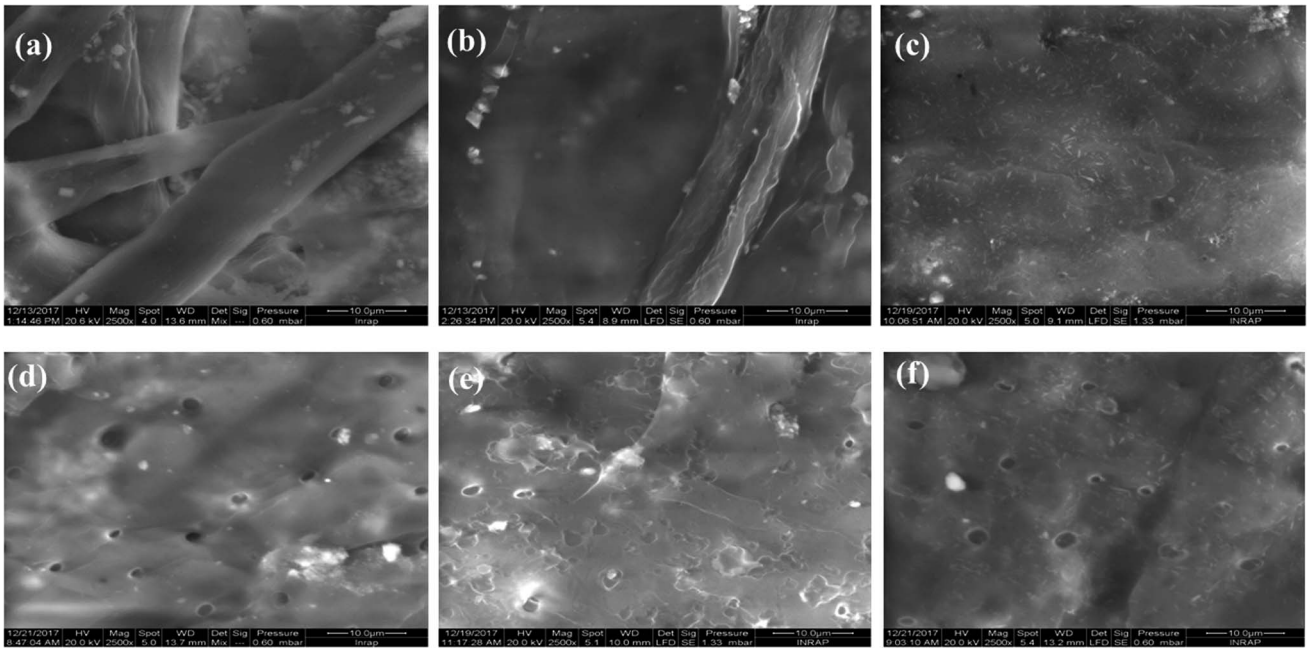

Fig. 5 Scanning electron microscopy images (×2500) of (a) uncoated paper, (b) paper coated with PVA, (c) paper coated with PVA/12 HNTs, (d) paper coated with PVA/25 BW, (e) paper coated with PVA/50 BW, and (f) paper coated with PVA/12 HNTs/50 BW.

the formation of hydrogen interactions between PVA, HNTs, and BW (as confirmed by FTIR analysis) which may limit the availability of hydroxyl groups on the coating surface and thus increase the hydrophobic performance of the PVA/HNTs/BW emulsified nanocomposite-based coatings.

Contact angle measurement. The effect of HNTs and/or BW contents on the hydrophobicity of the different coated paper samples was evaluated by the contact angle method. As it can be inferred from Table 5, no significant effect on contact angle values of PVA/HNTs nanocomposite coated paper samples was observed as a result of increasing HNTs content from 6 to 12 wt% as compared to both uncoated paper and paper coated with the pristine PVA polymer ($p > 0.05$), indicating a poor water resistance capability. This behavior is most likely due to the hydrophilic nature of HNTs which are reported to display, on their surface, negative charges that may attract water molecules.[50,51] In agreement with our results, noticeable changes in the wettability of sodium caseinate (NaCAS)/HNTs nanocomposite coated papers were observed as a result of increasing HNTs content from 0.73 to 5 wt%.[26] Conversely, Wang *et al.*[52] claimed an increase in the hydrophobicity of chitosan/montmorillonites nanocomposite coated papers when increasing montmorillonites (highly hydrophilic filler) contents from 0.1 to 0.3 wt% most likely due the increase in the surface roughness of the applied nanocomposite coatings. Similar trend was reported by Alakrach *et al.*[47] who noticed an increase in contact angle values of PLA-based films as a result of incorporating high HNTs loadings. According to these authors, the increase in the surface roughness of the hydrophobicity. On the other hand, increasing BW content from 25 to 50 wt% significantly increased the contact angle values of PVA/BW emulsified coated papers in the range of 13.62–22.15% as compared to the uncoated paper and the paper coated with pristine PVA ($p <$ 0.05), underlining the ability of the applied emulsified coatings to provide higher waterproof performance to the resulting emulsified coated papers. In agreement with our findings, a significant increase in the hydrophobicity of chitosan/BW coated paper was noticed by Zhang *et al.*[21] when BW content was increased from 30 to 90 wt%. Such increase in the water resistance of the emulsified coated papers can be explained by the hydrophobic characteristics of the incorporated BW along with its ability to re-solidify after the drying process, giving rise to the formation of a more continuous layer on the surface of the cellulosic material which may reduce its affinity towards water diffusion. Recently, Bang *et al.*,[53] noticed an increase in the contact angle value of carnauba wax-coated wood surface as compared to the uncoated wood raw material most likely due to the modification in the surface energy and roughness of the coating layer due to the presence of alkyl chains in carnauba wax composition. On the other hand, HNTS and BW co-incorporation at different contents significantly increased the contact angle values of PVA/HNTS/BW emulsified nanocomposite coated papers as compared to the uncoated paper, papers coated with pristine PVA and papers coated with PVA/HNTs nanocomposite-based coatings ($p < 0.05$). This increase was in the range of 10–20.44%. Since HNTs have a relatively hydrophilic characteristic compared to BW, such a reduction in the wettability of coated sheets is most likely due to the hydrophobicity of the incorporated wax along with the increase in the roughness of the applied coating which may increase water molecules pathway diffusion, leading to more hydrophobic material.[53]

WVP. Data related to changes in the WVP of coated paper as a function of HNTs and BW contents are presented in Table 5. As expected, due to its porous and hydrophilic nature, the uncoated paper material showed poor water vapor barrier

properties with a WVP value of 38.25 ± 0.26 g mm m^{-2} d^{-1} kPa^{-1}. In contrast, regardless of HNTs and BW contents, the water barrier properties of coated paper were significantly improved ($p < 0.05$) most likely due to the ability of the applied coatings to fill the porous structure of the cellulosic material. As it can be inferred from Table 5, no significant effect on WVP values of PVA/HNTs nanocomposite coated paper samples was noticed as a result of increasing HNTs content from 6 to 12% w/w as compared to paper coated with the pristine PVA film ($p > 0.05$) most likely due to the hydrophilic character of the incorporated nanofillers. In agreement with our results, no significant effect on the WVP of bagasse paper was observed by Hassan *et al.*[54] when applying a mixture of chitosan nanoparticles and nanofibrillated cellulose as coating materials on their surface. According to these authors, the incorporated nanoparticles may increase the spacing between the fibrils, leading to higher water vapor transmission through the resulting nanocomposites. Moreover, the presence of hydrophilic functional groups on the surface of the incorporated nanoparticles may accelerate the diffusion of water vapor molecules through the reinforced material, leading to a decrease in their water vapor barrier performance. On the other hand, increasing BW content to 50 wt% significantly reduced the WVP of PVA/BW emulsified coated papers by more than 20% as compared to the uncoated paper ($p < 0.05$). This result was expected as waxes were reported to be the most efficient compounds in reducing moisture permeability owing to their high hydrophobicity, which is mainly attributed to their high content of esters, long-chain fatty alcohols, acids, and long-chain alkanes.[55] In agreement with our findings, a reduction in the range of 54.10–96.70% was noticed in WVP of paper sheets upon the application of a microcrystalline wax emulsion on their surface.[48] Such an improvement in the water vapor performance of coated sheets was attributed to the strong hydrophobicity of the branched saturated hydrocarbons of C31-70 composing the microcrystalline wax. On the other hand, the observed reduction in the WVP of paper samples coated with PVA/6 HNTs/25 BW and PVA/6 HNTs/50 BW emulsified nanocomposite coatings as compared to papers coated with the pristine PVA film, was most likely due to the high hydrophobicity of the incorporated wax along with the increase in the roughness of the applied coatings, which may slow water vapor molecules diffusion, leading to lower WVP values.

Mechanical properties. Changes in the mechanical properties of coated papers as a function of HNTs and BW contents were evaluated in terms of tensile strength (TS) and elongation at break (% *E*) (Table 5).

Tensile strength (TS). As it can be inferred from Table 5, regardless of HNTs and BW contents, the application of the different coatings on the paper surface significantly increased the TS values of coated papers with respect to the uncoated cellulosic material ($p < 0.05$). Similarly, a significant increase in the range of 8.27–13.37% was noticed in the TS values of paper sheets coated with chitosan as compared to the uncoated paper, most likely due to the ability of chitosan particles to penetrate the interfibrillar space of the cellulosic matrix, leading to an increase in the bond strength of fibers and paper tenacity.[45] Likewise, Aloui and Khwaldia[26] reported a noticeable enhancement in the mechanical strength of papers coated with NaCas for which an increase in TS values from 19 to 47.89% was recorded when the coating weight was increased from 4.88 to 17 g m^{-2}. Such enhancement in the strength of coated papers was mainly ascribed to the ability of NaCas-based coatings to act as reinforcement layers on the paper surface. Interestingly, increasing HNTs content from 6 to 12 wt% increased the TS values of papers coated with PVA/HNTs nanocomposite-based films in the range of 12.03–23.79% as compared to the paper sample coated with pristine PVA ($p < 0.05$). Based on SEM and FTIR analysis, the observed reinforcing effect of HNTs on PVA/HNTs nanocomposite coated papers is most likely due to the good dispersion of HNTs in the PVA matrix along with the establishment of hydrogen interactions between the OH groups of PVA and the oxygen atoms of Si–O bonds or hydroxyl groups present on the surfaces of HNTs which may reinforce the cohesion of the polymeric matrix and thus boost the strength and tenacity of PVA/HNTs nanocomposite coated sheets. Our results corroborate those of Huang *et al.*[56] who noticed an increase in the tensile index of PVA/cellulose nanofibers coated paper when cellulose nanofibers (CNFs) content was increased to 3.0 wt%, most likely due to the ability of the incorporated CNFs to interact through their hydroxyl groups with fibers on the surface of paper leading to the enhancement of bonding force between the cellulosic fibers, thus improving the tensile strength of the resulting nanocomposite papers. Similar behavior was previously noticed by Mao *et al.*[57] who reported a percentage increase of 12.46% in the tensile index of nanocomposite multi-walled carbon nanotubes (MWCNTs)/polyaniline (PANI) nanocomposites coated paper as a result of increasing MWCNTs content as compared to the base paper. Such improvement in the mechanical strength of the resulting coated papers was mainly attributed to the excellent reinforcing effect of incorporating nanofillers along with the ability of MWCNTs and PANI to form a core–shell structure that may confer external force to the whole system, leading to the improvement of the mechanical properties of surface-coated paper. Likewise, a significant increase in the tensile index of polyaniline/cellulose nanocrystal (PANI/CNC) nanocomposite coated paper was reported by Huang *et al.*[58] when increasing CNC content from 2 to 8 wt%. This increase was in the range of 9.8 and 15.7% as compared to paper coated with pristine PANI. This result underlines the ability of the incorporated CNC to enhance the mechanical resistance of the resulting nanocomposite paper samples mainly due to their high modulus. In addition, such an improvement in the tenacity of the whole system was attributed to the strong interaction occurring between CNC and PANI, leading to the formation of a strong network structure that may increase the coating strength and thus the mechanical resistance of the coated paper. On the other hand, ANOVA analysis revealed that increasing BW content did not significantly affect the mechanical strength of PVA/BW emulsified coated papers as compared to paper coated with pristine PVA ($p > 0.05$). Previous studies have reported a significant reduction in the mechanical strength of paper treated with biopolymer-wax-based coatings.[45,55,59] As previously

explained by Khwaldia,[55] the decrease in mechanical strength of paper coated with polymer-wax-based formulations may be ascribed to the weakening effect exerted by these hydrophobic compounds on the polymeric network. In fact, it has been reported that interactions between nonpolar molecules such as waxes and polar polymers are much weaker than those between polymer–polymer molecules, which may result in poor tensile properties.[41] Overall, the effect of lipid addition on the mechanical strength of hydrocolloid-based films and coatings depends on different factors including the nature, the amount, and the physical state of the lipid phase, as well as the type of the polymer and the film fabrication process.[41] On the other hand, HNTs and BW incorporation at different loadings slightly increased the TS values of PVA/HNTs/BW emulsified nanocomposite coated paper samples as compared to papers treated with PVA/BW and paper coated with pristine PVA most likely due to the reinforcing effect of HNTs (as explained previously) along with the establishment of interactions between PVA, BW, and HNTs as confirmed by FTIR analysis.

Elongation at break (% E). As it can be inferred from Table 5, regardless of HNTs and BW contents, a significant increase in the range of 27.36–41.43% was noticed in the % *E* of coated paper as compared to the uncoated cellulosic material, underscoring the ability of the applied coatings to improve the flexibility of the paper material ($p < 0.05$). Similarly, Aloui and Khwaldia[26] reported an increase in the plastic response of NaCas-coated paper when the coating weight was increased from 4.88 to 17 g m^{-2}. Such enhancement in the plastic response of coated paper was attributed to the stress relaxation occurring in the cellulosic material as a result of its exposure to the applied humid coating solution during the coating process. Regardless of nanofiller content, HNTs incorporation did not let to any significant changes in the % *E* of PVA/HNTs coated paper as compared to paper coated with the pristine PVA ($p > 0.05$). Our results corroborate those of Shen *et al.*[6] who did not notice any significant effect on the flexibility of PVA/alkyl ketene dimer/HNTs coated paper when increasing HNTs content from 3 to 10 wt%. Conversely, an enhancement in the flexibility of NaCas/HNTs nanocomposite coated paper was noticed by Aloui and Khwaldia[26] when HNTs content was increased from 0.73 to 5 wt%. This improvement was mainly ascribed to the plasticizing effect of HNTs as hydrophilic fillers. On the other hand, no significant effect on % *E* of PVA/BW coated paper was noticed as a result of increasing BW content from 25 to 50 wt% as compared to paper coated with pure PVA ($p > 0.05$). Previously, Khwaldia[55] noticed a decrease in the % *E* of paper coated with NaCas/paraffin-based coatings as a result of increasing paraffin wax content to 20–40 wt%. Such a decrease in the flexibility of the emulsified coated paper was attributed to the presence of lipid globules that may affect the continuity of the protein network. Conversely, many studies have noticed an enhancement in the plastic response of bio-based films upon wax incorporation most likely due to the plasticizer effect of the lipid phase wax.[60] On the other hand, HNTS and BW co-incorporation at different loadings slightly decreased the % *E* of PVA/HNTs/BW emulsified nanocomposite-coated paper samples as compared to paper coated with pristine PVA ($p < 0.05$), due to the increase in the rigidity of the applied nanocomposite-based coatings, which is mainly ascribed to the ability of HNTs to form strong interfacial interactions with the PVA matrix. Conversely, Klangmuang and Sothornvit[25] did not reveal any significant improvement in the flexibility of HPMC/MMT nanocomposite film upon BW incorporation, most likely because the incorporated amount was sufficient to maintain the mechanical properties of the original HPMC film.

Conclusion

Novel emulsified nanocomposite films based on PVA incorporating different loadings of HNTs and BW were successfully developed and applied to paper sheets to enhance their functional properties. Interestingly, the co-incorporation of HNTs and BW significantly improved the barrier properties and the tensile strength of the resulting emulsified nanocomposite-coated paper samples. Owing to their ability to combine the prominent reinforcement effects of nanofillers with the excellent moisture–barrier properties of hydrophobic compounds, the developed nanocomposite emulsified papers can be used as promising primary packaging systems for dry food products (*e.g.* cereals, biscuits, bread and baked products, tea, coffee and sugar) and fresh produces (*e.g.* fruits and vegetables).

Conflicts of interest

The authors declare no conflicts of interest.

Acknowledgements

This work was supported by the Tunisian Ministry of Higher Education and Scientific Research, Grant/Award Number: LR15INRAP02. The authors would like to thank all INRAP technical staff for their collaboration.

Notes and references

1 W. Wang, F. Gu, Z. Deng, Y. Zhu, J. Zhu, T. Guo, J. Song and H. Xiao, *Carbohydr. Polym.*, 2020, **255**, 117431.
2 P. K. Kunam, D. Ramakanth, K. Akhila and K. K. Gaikwad, *Biomass Convers. Biorefin.*, 2022, **2022**, 1–16.
3 H. Chen, B. Wang, J. Li, G. Ying and K. Chen, *Carbohydr. Polym.*, 2022, **288**, 119371.
4 A. Adibi, D. Valdesueiro, L. Simon, C. P. Lenges and T. H. Mekonnen, *ACS Sustain. Chem. Eng.*, 2022, **10**, 10718–10732.
5 B. Liu, J. Zhang and H. Guo, *Membranes*, 2022, **12**, 347.
6 Z. Shen, A. Rajabi-Abhari, K. Oh, G. Yang, H. J. Youn and H. L. Lee, *Polymers*, 2021, **13**(8), 1334.
7 M. C. Condés, M. C. Añón, A. Dufresne and A. N. Mauri, *Food Hydrocolloids*, 2018, **74**, 159–167.
8 J. Pires, C. D. de Paula, V. G. L. Souza, A. L. Fernando and I. Coelhoso, *Polymers*, 2021, **13**, 1–29.
9 H. L. Calambas, A. Fonseca, D. Adames, Y. Aguirre-Loredo, C. Caicedo and D. A. Co, *Molecules*, 2021, **26**, 6734.

10 C. A. Díaz-Cruz, C. Caicedo, E. J. Jiménez-Regalado, R. Díaz de León, R. López-González and R. Y. Aguirre-Loredo, *Polymers*, 2022, **14**(11), 2166.
11 Y. Zhang, A. Tang, H. Yang and J. Ouyang, *Appl. Clay Sci.*, 2016, **119**, 8–17.
12 H. Aloui, K. Khwaldia, M. Hamdi, E. Fortunati, J. M. Kenny, G. G. Buonocore and M. Lavorgna, *ACS Sustain. Chem. Eng.*, 2016, **4**, 794–800.
13 W. Kajthunyakarn, R. Khlibsuwan, D. Sakloetsakun and T. Pongjanyakul, *J. Drug Delivery Sci. Technol.*, 2019, **54**, 101235.
14 L. Lisuzzo, G. Cavallaro, S. Milioto and G. Lazzara, *Appl. Clay Sci.*, 2020, **185**, 105416.
15 N. P. Risyon, S. H. Othman, R. K. Basha and R. A. Talib, *Food Packag. Shelf Life*, 2020, **23**, 100450.
16 K. Khwaldia, S. Banon, C. Perez and S. Desobry, *J. Dairy Sci.*, 2004, **87**, 2011–2016.
17 F. K. G. Dos Santos, K. N. De Oliveira Silva, T. D. N. Xavier, R. H. De Lima Leite and E. M. M. Aroucha, *Mater. Res.*, 2017, **20**, 485–491.
18 S. Galus, M. Gaouditz, H. Kowalska and F. Debeaufort, *Int. J. Mol. Sci.*, 2020, **21**, 1–19.
19 J. Salvada, B. Alke, C. Brazinha, V. D. Alves and I. M. Coelhoso, *Coatings*, 2022, **12**(6), 813.
20 R. Sothornvit, *Food Res. Int.*, 2009, **42**, 307–311.
21 W. Zhang, H. Xiao and L. Qian, *Appl. Surf. Sci.*, 2014, **300**, 80–85.
22 Y. Wang, X. Zhang, L. Kan, F. Shen, H. Ling and X. Wang, *Green Chem.*, 2022, **24**, 7039–7048.
23 A. R. A. Hammam, *SN Appl. Sci.*, 2019, **1**, 1–11.
24 P. Klangmuang and R. Sothornvit, *Food Hydrocolloids*, 2016, **61**, 609–616.
25 P. Klangmuang and R. Sothornvit, *Lebensm.-Wiss. Technol.*, 2016, **65**, 222–227.
26 H. Aloui and K. Khwaldia, *Cellulose*, 2017, **24**, 4493–4507.
27 ISO 535, *Determination of water absorptiveness — Cobb method*, International Organization of Standardization, Geneva, Switzerland, 2014.
28 H. Aloui, F. Licciardello, K. Khwaldia, M. Hamdi and C. Restuccia, *Int. J. Food Microbiol.*, 2015, **200**, 22–30.
29 ISO 2528, *Determination of water vapour transmission rate (WVTR) — Gravimetric (dish) method*, International Organization for Standardization, Geneva, Switzerland, 2017.
30 K. Khwaldia, A. H. Basta, H. Aloui and H. El-Saied, *Carbohydr. Polym.*, 2014, **99**, 508–516.
31 T. S. Gaaz, A. B. Sulong, A. A. H. Kadhum, A. A. Al-Amiery, M. H. Nassir and A. H. Jaaz, *Molecules*, 2017, **22**, 13–15.
32 Y. Zhang, X. He, J. Ouyang and H. Yang, *Sci. Rep.*, 2013, **3**, 1–6.
33 Z. W. Abdullah and Y. Dong, *J. Mater. Sci.*, 2018, **53**, 3455–3469.
34 A. Ghebaur, S. Alexandra Garea, S. Cecoltan and H. Iovu, *Mater. Plast.*, 2017, **54**, 8–13.
35 M. Mousa and Y. Dong, *Polymers*, 2020, **12**(2), 264, DOI: **10.3390/polym12020264**.
36 T. L. Nguyen, H. T. Nguyen, V. K. Nguyen, T. T. H. Pham, T. H. T. Le and T. T. Nguyen, *Key Eng. Mater.*, 2020, **850**, 87–93.
37 Y. Zhang, B. K. Simpson and M. J. Dumont, *Food Biosci.*, 2018, **26**, 88–95.
38 Y. H. Wen, C. H. Tsou, M. R. de Guzman, D. Huang, Y. Q. Yu, C. Gao, X. M. Zhang, J. Du, Y. T. Zheng, H. Zhu and Z. H. Wang, *Polym. Bull.*, 2022, **79**, 3847–3866.
39 G. Liu, Y. Song, J. Wang, H. Zhuang, L. Ma, C. Li, Y. Liu and J. Zhang, *Lebensm.-Wiss. Technol.*, 2014, **57**, 562–568.
40 M. Liu, B. Guo, M. Du and D. Jia, *Appl. Phys. A: Mater. Sci. Process.*, 2007, **88**, 391–395.
41 M. A. Haq, A. Hasnain, F. A. Jafri, M. F. Akbar and A. Khan, *Lebensm.-Wiss. Technol.*, 2016, **68**, 674–680.
42 S. Sinaringati, N. Putra, M. Amin and F. Afriyanti, *ARPN J. Eng. Appl. Sci.*, 2016, **11**, 800–804.
43 D. Kim, I. Park, J. Seo, H. Han and W. Jang, *J. Polym. Res.*, 2015, **22**(2), DOI: **10.1007/s10965-014-0650-x**.
44 M. Sultan, O. M. Hafez, M. A. Saleh and A. M. Youssef, *RSC Adv.*, 2021, **11**, 9572–9585.
45 A. Bhardwaj, N. Sharma, T. Alam, V. Sharma, J. K. Sahu, H. Hamid, V. Bansal and M. S. Alam, *Waste Biomass Valorization*, 2023, **14**, 1625–1636, DOI: **10.1007/s12649-022-01952-1**.
46 D. Kansal, S. S. Hamdani, R. Ping and M. Rabnawaz, *Ind. Eng. Chem. Res.*, 2020, **59**, 12075–12084.
47 A. M. Alakrach, N. Z. Noriman, O. S. Dahham, A. A. Al-Rashdi, I. Johari, Z. M. Razlan, A. B. Shahriman, I. Zunaidi and W. Khairunizam, *IOP Conf. Ser.: Mater. Sci. Eng.*, 2019, **557**, 012067.
48 H. Türe, M. Gällstedt, E. Johansson and M. S. Hedenqvist, *Ind. Crops Prod.*, 2013, **51**, 1–6.
49 D. Liu, Y. Duan, S. Wang, M. Gong and H. Dai, *Polymers*, 2022, **14**(9), 1786.
50 G. Stoclet, M. Sclavons, B. Lecouvet, J. Devaux, P. Van Velthem, A. Boborodea, S. Bourbigot and N. Sallem-Idrissi, *RSC Adv.*, 2014, **4**, 57553–57563.
51 M. J. Saif and H. M. Asif, *J. Chil. Chem. Soc.*, 2015, **60**, 2949–2953.
52 K. Wang, L. Zhao and B. He, *Polymers*, 2021, **13**, 1607.
53 J. Bang, J. Kim, Y. Kim, J. K. Oh, H. Yeo and H. W. Kwak, *J. Korean Wood Sci. Technol.*, 2022, **50**, 149–158.
54 E. A. Hassan, M. L. Hassan, R. E. Abou-zeid and N. A. El-Wakil, *Ind. Crops Prod.*, 2016, **93**, 219–226.
55 K. Khwaldia, *J. Food Biochem.*, 2010, **34**, 998–1013.
56 S. Huang, X. Wang, Y. Zhang, Y. Meng, F. Hua and X. Xia, *Sci. Rep.*, 2022, **12**, 1–10.
57 T. Mao, Y. Tang, Y. Zhang, J. Zhang and D. Guo, *J. Appl. Polym. Sci.*, 2018, **135**(23), 46329.
58 M. Huang, Y. Tang, X. Wang, P. Zhu, T. Chen and Y. Zhou, *Prog. Org. Coat.*, 2022, **159**, 106452, DOI: **10.1016/j.porgcoat.2021.106452**.
59 N. Hendrawati, A. A. Wibowo, R. D. Chrisnandari and R. Adawiyah, *IOP Conf. Ser.: Mater. Sci. Eng.*, 2021, **1073**, 012006.
60 S. Nurul Syahida, Z. M. A. Ainun, M. R. Ismail-Fitry and Z. A. Nur Hanani, *Packag. Technol. Sci.*, 2020, **33**, 417–431.